Nature Nanotechnology 5, 345 - 349 (2010)
Published online: 11 April 2010 | doi:10.1038/nnano.2010.56

Subject Categories: Nanoparticles | Photonic structures and devices

Observation and control of blinking nitrogen-vacancy centres in discrete nanodiamonds

C. Bradac[1,2], T. Gaebel[1,2], N. Naidoo[1], M. J. Sellars[3], J. Twamley[1], L. J. Brown[4], A. S. Barnard[5], T. Plakhotnik[6], A. V. Zvyagin[2] & J. R. Rabeau[1,2]

Abstract

Nitrogen-vacancy colour centres in diamond can undergo strong, spin-sensitive optical transitions under ambient conditions, which makes them attractive for applications in quantum optics[1], nanoscale magnetometry[2,3] and biolabelling[4]. Although nitrogen-vacancy centres have been observed in aggregated detonation nanodiamonds[5] and milled nanodiamonds[6], they have not been observed in very small isolated nanodiamonds[7]. Here, we report the first direct observation of nitrogen-vacancy centres in discrete 5-nm nanodiamonds at room temperature, including evidence for intermittency in the luminescence (blinking) from the nanodiamonds. We also show that it is possible to control this blinking by modifying the surface of the nanodiamonds.

Introduction

Detonation nanodiamond is routinely produced on an industrial scale, and the raw material can be disintegrated into a stable 5-nm monodisperse colloid[8]. The combination of inert core and chemically reactive surface, which can host a variety of moieties, is appealing for chemists, biologists and material scientists[9,10]. Quantum magnetometry[2,3] is an example of an emerging technology that will directly benefit from the availability of nanocrystals with well-defined sizes in the 5-nm range, because the sensitivity to single spins is inversely proportional to the cube of the distance between the sensor (that is, the nitrogen-vacancy (NV) centre) and the spin being detected.

Producing and detecting NV colour centres in isolated 5-nm detonation nanodiamond has been controversial, and there has been some scepticism regarding their stability as a useful emitter in a discrete crystal. For example, theoretical calculations of the crystal energy budget favour the location of nitrogen on the surface rather than in the core, which seems to explain the limited observation of NV centres in chemical vapour deposition and high-pressure high-temperature grains of less than 40 nm in size[11,12], and favours the prediction that nanodiamonds smaller than 10 nm in size do not contain NV centres[7,13]. Although sub-10-nm nanodiamonds with NV centres

have been produced using a top-down approach (milling luminescent high-pressure high-temperature microdiamonds into 7-nm particles[6,14]), the question of NV stability in isolated detonation nanodiamonds persists.

In aggregated detonation nanodiamonds (agglomerates and agglutinates[8]), high-sensitivity, time-gated luminescence and electronic paramagnetic resonance spectroscopy have been used to extract a weak NV signal from a strong luminescence background[5]. The experiments highlight the eclipsing nature of the graphitic surface layers in nanodiamond aggregates—NV centres were simply not visible through the broadband luminescence from the surface and grain boundary material. To distinguish the NV spectral signature from the large grain boundary luminescence overhead, diamond synthesis yielding discrete sub-10-nm detonation nanodiamonds is vital. Here, we use a robust deaggregation and dispersion method, which diminishes the crystal–crystal interaction to yield a quasi-isolated system of 'free-space' crystals weakly coupled to the underlying substrate. In contrast to other materials and processing techniques (such as milling[6,14]), this method produces isolated detonation nanodiamonds with a well-defined size distribution on a dry substrate (see Methods).

Figure 1 presents data from the analysed sample, collected with the combined confocal scanning fluorescence and atomic force microscope (AFM) system described previously[11] (a schematic is shown in Supplementary Fig. S1). The laser excitation power was 300 μW. The AFM-based measurements clearly show areas of the sample showing a sparse spatial distribution of nanoparticles (Fig. 1a) with a typical size in the 5 nm range (Fig. 1c). We also carried out transmission electron microscopy (TEM) observations to further quantify the size of the nanodiamond crystals (detailed in Supplementary Information). As shown, some isolated nanoparticles (~1%) were luminescent (Fig. 1b), and their spectra (Fig. 1d) were consistent with those reported for NVs in nanodiamonds[6,14]. Furthermore, the second-order correlation function[1] $g^{(2)}(t)$ (see Methods) confirmed that the emission originated from a single centre (Fig. 1d, inset). The emission lifetime varied from 2 to 14 ns, with a mean value of ~5.5 ns. There was no observed difference in the distribution of lifetimes for blinking and non-blinking centres. Further studies are required to understand the quenching mechanism, which favours a shorter lifetime. It has been shown recently that NV centres in a detonation-nanodiamond host show a bi-exponential decay, with time constants of 2.5 and 20 ns[15], the shortened lifetime being attributed to quenching from surface graphite.

Figure 1: Characterization of discrete 5-nm diamonds on a glass coverslip.

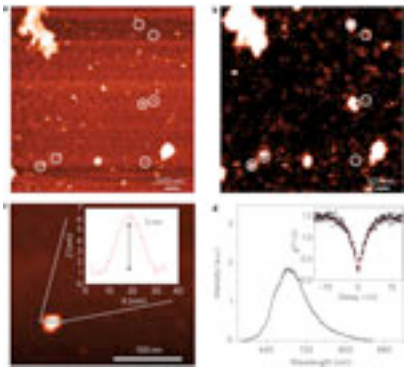

a, AFM image of nanodiamonds. The brightness of the spots is proportional to the height of the crystals (circles highlight the correspondence between the AFM image and the confocal image of **b**). **b**, Corresponding confocal

scanning fluorescence microscopy image. Bright spots indicate NV emitters. **c**, Magnified AFM image and corresponding surface profile (inset) of a representative nanocrystal 5 nm in height. **d**, Emission spectrum of an NV centre in a 5-nm crystal host and corresponding second-order correlation function $g^{(2)}$ (inset).

Additional confirmation of the existence of NV centres in the as-received nanodiamond sample was obtained by performing optically detected magnetic resonance (ODMR) to probe the well-characterized ground-state triplet splitting. In previous studies, nanodiamond-hosted NV centres have been shown to have a zero-magnetic-field, strain-related splitting[6], in excellent agreement with the ODMR spectrum shown in Fig. 2b, which represents an unambiguous signature of NV centres in the detonation nanodiamond. The luminescence spectrum was centred at 650 nm, in agreement with that reported by Smith and colleagues[5], and probably included a strong sp^2-bonded carbon luminescence from the grain boundary of the nanodiamond agglomerates, which overshadowed the NV luminescence (centred at 700 nm, compare with Fig. 1d), but not the ODMR signal. ODMR was undetectable with our apparatus in the free-space nanodiamonds. We attribute this to strong dephasing owing to the distorted crystal order and a weak signal exacerbated by the reduced count rate due to blinking.

Figure 2: Luminescence and magnetic resonance spectra from detonation nanodiamond.

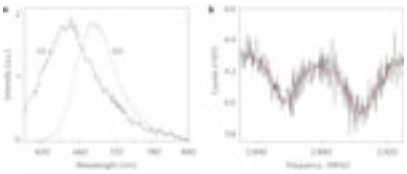

a, Representative NV centre spectra, as acquired in nanodiamonds incorporated in aggregates and/or a PVA film (i) and in the free-space sample (ii). **b**, Optically detected magnetic resonance spectrum associated with the luminescence spectrum (i), showing the two characteristic magnetic resonance dips indicating a strain-induced splitting of the $m_s = \pm 1$ spin sublevels typical of NV centres in nanodiamonds.

The observation of luminescence from single, isolated NV centres in 5-nm detonation nanodiamonds, which has been the subject of intense debate, is important because, until now, luminescence from ~5-nm crystals has been observed only in detonation nanodiamond agglomerates[5]. Furthermore, and in contrast to agglomerates (where the diamond surface is largely encased), we also observed a new property of NV centres: luminescence intermittency or 'blinking'. NV has been described as an extremely photostable emitter immune to bleaching[1] or blinking, as represented by a typical luminescence time trajectory (Fig. 3a) acquired in a sample prepared using the polyvinyl alcohol (PVA) polymer sample preparation method[6].

Figure 3: Detailed analysis of blinking statistics from an NV centre in detonation nanodiamond.

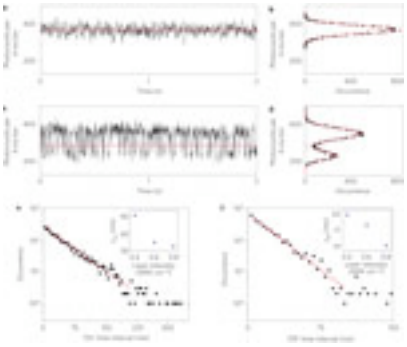

a–**d**, A 2-s fragment of a 200-s luminescence time trajectory of the NV centres sampled into 4-ms bins from two separate diamond samples: NV luminescence from nanodiamonds embedded in a PVA polymer film (**a**), with corresponding histogram fitted with a single Gaussian (**b**), where the line in **a** is the mean count rate; a single isolated NV in nanodiamond displaying intermittent luminescence (**c**), with corresponding histogram of the full time trajectory fitted with two Gaussians (**d**). Gaussians are fitted to the 'on' and 'off' state photon distributions and a line is drawn through **c** to indicate the on/off 'threshold' for analysing the emission statistics. **e**,**f**, Blinking statistics of the 'on' and 'off' states on a semi-logarithmic scale (symbols). A single exponential is fitted in both cases, with time constants 45 and 18 ms, respectively. Insets to **e** and **f** plot blinking time constant versus the excitation laser intensities for 'on' and 'off' states, respectively.

Figure 3c shows a representative blinking luminescence time trajectory from a nanodiamond containing an NV centre, in which the diamonds were prepared as described in the Methods. Blinking was observed in ~25% of the luminescent sites. The 'off' state was at the level of the background signal, and blinking due to photochromism[16] was ruled out as the neutral NV luminescence signature was never observed in the spectra. Photobleaching was also observed on some of the centres; however, those analysed in this Letter showed luminescence over several hours of illumination. We analysed blinking by sampling the luminescence time trajectories at 4-ms time bins and analysed the data using accepted signal-processing algorithms, in which the position of the signal relative to a threshold level determines the assignment of the states[17]. The blinking phenomena were also characterized as a function of the excitation intensity (shown in the insets of Fig. 3e,f, and detailed in the Supplementary Information).

The 4-ms bin width was chosen because it provides the deepest minimum between the two Gaussian curves shown in Fig. 3d. Averaging data into 4-ms bins on the one hand ignores the rapid events that may display complex dynamics[18], but on the other hand decreases the noise and emphasizes the two-state NV-nanodiamond blinking system, as shown in Fig. 3d. Changing the bin time to 2 ms did not change the result, and with 1-ms bins the statistical noise was too pronounced for a meaningful result. These two states are identified as 'on' and 'off'[19]. Quantum dots[20], single molecules[21], silicon nanocrystals in a porous silicon matrix[22] and others[23] are well-known systems that show blinking. The validity of the two-state on/off model is intensely debated[24], especially in the context of quantum-dot studies, where, for example, three states[25] and a continuous distribution of states[26] have been reported. In our case, the validity of the two-state model was underpinned by the photon distribution in 'on' and 'off' states based on the Gaussian distribution and expressed as

$$P(N) = \frac{p_{on}}{\sqrt{2\pi}\sigma_{on}} \exp\left[-\frac{\left(N-\bar{N}_{on}\right)^2}{2\sigma_{on}^2}\right] + \frac{p_{off}}{\sqrt{2\pi}\sigma_{off}} \exp\left[-\frac{\left(N-\bar{N}_{off}\right)^2}{2\sigma_{off}^2}\right]$$

where $\bar{N}$ represents the mean value of the number of photons in each state, p is the population of the states, N the total number of photons and σ^2 the variance of the distribution. For a stable photon emission, the variance equals the mean value. The fit to the distribution reveals σ_{on}^2 to be only about two times larger than the mean $\bar{N}_{on}$. This determined our choice of the threshold level between the 'on' and 'off' states, which was set at the intersection of the two Gaussians (Fig. 3c,d), where the probabilities for N to be at the 'on' and 'off' levels were equal. The distribution of the 'on' and 'off' times are plotted on a semi-logarithmic scale in Fig. 3e,f, together with the data-fitting curves, which display exponential trends in both the 'on' and 'off' cases.

We now discuss blinking mechanisms in the context of other well-studied systems. Passivated quantum dots and single molecules in polymer matrices are examples of trap-abundant quantum systems that show blinking. It has been shown that removing traps from the passivated quantum-dot surface suppresses blinking[23]. In general, excitation/emission is mediated by an exciton, (that is, charge separation, where the electron determines the kinetics of this process by virtue of its higher mobility). It is the capture of this electron by (surface) traps that inhibits exciton recombination (switching the emitter to the 'off' state) where the trap-abundant matrix disorder promotes this capture[23]. The optical excitation/emission process in an NV centre is also mediated by an exciton. However, the NV defect-associated exciton is bound, or localized at the NV site, within the Bohr radius (<1 nm), unlike the case for quantum dots, where an exciton is essentially delocalized. In the case of NVs in ~5-nm detonation nanodiamonds, the blinking may therefore be a manifestation of the local crystal disorder. An NV centre is situated in a ~5-nm crystal comprising a crystalline diamond core sized 2–3 nm and a mixed sp^2–sp^3 hybridization shell of quasi-spherical shape[27] distorted by the large proportion of surface dangling bonds (~20% of total carbon atoms)[28], dislocations[29] and impurities. The outer shell has been found to regain some sp^3 hybridization by surface passivation, for example, with oxygen-containing moieties[28, 30], as in the present study. Owing to the proximity of the NV centre to the nanodiamond surface, it is also a possibility that surface functional groups and/or adsorbed species may also be a source of traps causing blinking.

To assess the degree of disorder in a typical nanodiamond, we carried out a series of density functional tight binding (DFTB) simulations on a model truncated octahedral structure, with all surfaces fully passivated with hydrogen atoms ($C_{837}H_{252}$). NV defects were individually inserted into over 50 unique lattice sites within the particle, as shown in Fig. 4a and described in the Supplementary Information. A number of parameters were used to assess the local crystal disorder at these sites, including the change in the average C–N bond length (Δd), as

shown in Fig. 4b. When sufficient disorder is present, there will be a shift in the electronic states, so the change in the energy of the lowest unoccupied molecular orbital (ΔE_{LUMO}) was also considered, as shown in Fig. 4c. In these and other cases (see Supplementary Information), the disorder is extreme when the site is within the excitonic radius (R_{Bohr}) from the surfaces, edges and corners (closed symbols), and NV centres within the core of the particle (where disorder is absent or insignificant) are the only centres that are likely to be optically active (open symbols in Fig. 4b,c). More details on the theoretical modelling are available in the Supplementary Information.

Figure 4: Theoretical characterization of the structural and electronic disorder.

a, Nanodiamond model, with all NV sites shown simultaneously (blue). **b**, Site-dependent change in the average C–N bond length (Δd). **c**, Site-dependent change in the energy of the lowest unoccupied molecular orbital (ΔE_{LUMO}). Closed symbols denote NV centres located within a Bohr excitonic radius from surfaces/edges/corners (where the surface/edge/corner is at 1 or –1 with respect to the centrosymmetric atom at the origin), where atoms with mixed hybridization reside, and open symbols indicate NV centres located beyond the excitonic radius from surfaces/edges/corners (that is, within the core, where atoms are entirely sp^3-hybridized).

Full size image (28 KB)

It is important to note that when these 5-nm diamonds were combined into aggregates and/or embedded in a polymer PVA film, electronic discontinuity at the interface was altered, and the individual NV-centre luminescence temporal behaviour was restored to a continuous luminescence signal, with no exceptions (Fig. 3a). This result reproduced previous reports on NV luminescence in nanodiamonds[4, 5, 12, 14]. However, in free space, discrete 5-nm nanodiamonds containing an NV centre revealed a new luminescence intermittency pattern, for which the effect of the nanodiamond surface state (as in the aggregated or polymer-embedded state) warrants further study.

This insight into the properties of NV centres in discrete nanodiamonds, as reported here, may affect a range of applications in the physical and life sciences. The presence or absence of blinking in nanodiamonds provides information about the local and surrounding environment of the hosted NV centre, which could find use in a variety of quantum or biosensing technologies. For example, harnessing the environmental sensitivity of blinking may enable the optical detection of changes in the surface functionalization of a nanodiamond probe.

Methods

Detonation diamond nanocrystals (as received, Diamond Technologies and Materials) with an average size of 5 nm, as measured by dynamic light scattering (not shown), were used for the experiments. The diamonds were processed using strong acid reflux and ultrasonication[31, 32], as outlined below.

The preparation of the nanodiamonds included a number of previously reported methods[31, 32], and was modified for optimal deagglomeration. It is worth mentioning that thermal oxidation can yield disperse sub-10-nm

nanodiamond crystals on lacey carbon, as reported previously[28]. Nanodiamonds were mixed with sulphuric acid (98%, 9 ml) and nitric acid (70%, 1 ml) and then refluxed for 3 days at 70 °C. The mixture was centrifuged and ultrasonicated, then refluxed again with a fresh acid mixture. Nanodiamonds were washed with Milli-Q® then refluxed with NaOH (0.1 M, 8 ml; 1 h, 90 °C), washed, then refluxed with HCl (0.1 M, 8 ml). The nanodiamond–acid mixture was washed with Milli-Q® and ultrasonicated (1 h). The sample was diluted by addition of Milli-Q (~20 ml) and ultracentrifuged (1 h, 100,000*g*). This procedure was repeated three times, and the resulting supernatant containing individual diamond grains was used for these experiments. Nanodiamonds were either dropped onto a glass coverslip and left to dry, or spin-coated. The compositions of the treated and untreated diamond were assessed by Raman spectroscopy (see Supplementary Information), showing a dramatic decrease in the graphitic compared with diamond content of the sample.

To embed nanodiamonds in a PVA film, they were mixed, in different proportions, with a 0.25% solution of PVA in de-ionized water. Two different molecular weight PVAs were used: average M_w, 85,000–24,000 (Aldrich 363146); average M_w, 31,000–50,000 (Aldrich 363138).

The agglomerated nanodiamonds were measured using optical microscopy and AFM-zooming on the regions of clear aggregation. Simultaneous topographic and luminescence imaging of the same sample area was carried out using a 'home-built', room-temperature confocal scanning fluorescence microscope (×100 oil-immersion objective lens, NA 1.4) illuminated with a continuous-wave 532-nm diode-pumped solid-state laser (Coherent, model: Compass 315M-100), combined with a commercial AFM (NT-MDT Ntegra) as described elsewhere[11]. The luminescence spectrum was acquired using a spectrometer (Princeton Instruments Acton 2500i, Camera Pixis 100 model: 7515-0001). A Hanbury Brown and Twiss interferometer was used to measure the second-order correlation function $g^{(2)}(\tau) = \langle I(t)I(t+\tau)/I(t)^2 \rangle$, where I is the luminescence signal intensity. The number of emitters per individual illuminated nanocrystal was determined by analysing $g^{(2)}$ at $\tau = 0$ and $\tau = \infty$, where $g^{(2)}(\tau = 0)$ is the probability of detecting two simultaneous photons normalized by the probability of detecting two photons at once for a random photon source. Because a single quantum system, such as a single NV centre, cannot simultaneously emit two photons at a time, $g^{(2)}(\tau = 0) = 0$, yielding an 'antibunching' dip otherwise governed by the sub-Poissonian statistics of the emitted photons. The $g^{(2)}$-contrast reports on the number of sampled emitters N_e, because it scales as $1/N_e$ (ref. 1).

ODMR interrogation of the single NV centres was designed and carried out using the accepted quantum-mechanical representation of an NV centre. The centre represents a two-level quantum system, which can be pumped to the first allowed energy level (excited state) by 532-nm laser excitation. The NV triplet ground energy levels with magnetic quantum numbers $m_s = 0$ and $m_s = \pm 1$ are split by spin–spin interaction by ~2.88 GHz. The cyclic luminescence of the $m_s = \pm 1$ excited state is 30% less efficient than that of the $m_s = 0$ excited state. The optical pumping populates the $m_s = 0$ ground state, thereby spin-polarizing the NV centre. Microwave radiation (2.88 GHz) mixes two ground states, thus causing a decrease in the luminescence signal, which represents an unambiguous fingerprint for the NV centre[33]. The microwave probe signal (0.2–0.6 mW) from a signal generator (Rohde & Schwarz SMIQ 06B, 300 kHz to 6.4 GHz) was radiated through a 20-μm copper wire situated on the sample substrate in sub-millimetre proximity to the probed NV centre. The observed ODMR spectrum featured two peaks, indicating lifting of the $m_s = \pm 1$ degeneracy, which was recognized to be strain-induced in nanodiamonds[6].

Theoretical simulations were performed using the density-functional-based tight-binding method with self-consistent charges (SCC-DFTB)[34], which is a two-centre approach to density functional theory, where the Kohn–Sham density functional is expanded to second order around a reference electron density. The reference density was obtained from self-consistent density functional calculations of weakly confined neutral atoms, and the confinement potential was optimized to anticipate the charge density and effective potential in molecules and solids. This method has the advantage of being non-periodic, and has previously been shown to be suitable for studying the crystallinity of diamond nanoparticles[35] and the distribution of substitutional nitrogen[7]. In the present study, all test structures were fully relaxed using the conjugate gradient scheme to minimize the total energy. The convergence criterion for a stationary point was 10^{-4} a.u. ≈ 5 meV Å^{-1} for forces.

Acknowledgements

The authors would like to thank N. Manson and F. Treussart for useful discussions, D. Birch for TEM measurements and E. Carter for Raman spectroscopy measurements. T.G. is funded by a Macquarie University Research Fellowship, C.B. is funded by a Macquarie University Research Excellence Scholarship, and J.R.R is funded by an ARC Future Fellowship. The work was funded in part by the Australian Research Council (DP0772286 and DP0771676).

Author Contributions

C.B., T.G., A.V.Z. and J.R.R. conceived and designed the experiments, analysed the data, contributed materials/analysis tools and co-wrote the paper. T.P. analysed the data and contributed analysis tools. M.J.S. contributed ESR equipment and expertise. A.S.B. carried out DFTB simulations and analysed simulation data. N.N., J.T., L.B. and J.R.R. designed the deaggregation protocol. N.N. prepared the nanodiamond samples. All authors discussed the results and commented on the manuscript.

Competing interests statement

The authors declare no competing financial interests.

Received 15 January 2010; Accepted 1 March 2010; Published online 11 April 2010.

References

1. Kurtsiefer, C., Mayer, S., Zarda, P. & Weinfurter, H. Stable solid-state source of single photons. Phys. Rev. Lett. 85, 290–293 (2000).
| Article | PubMed | ISI | ChemPort |
2. Balasubramanian, G. *et al*. Nanoscale imaging magnetometry with diamond spins under ambient conditions. Nature 455, 648–651 (2008).
| Article | PubMed | ChemPort |
3. Maze, J. R. *et al*. Nanoscale magnetic sensing with an individual electronic spin in diamond. Nature 455, 644–647 (2008).
| Article | PubMed | ChemPort |

4. Chang, Y.-R. *et al*. Mass production and dynamic imaging of fluorescent nanodiamonds. Nature Nanotech. 3, 284–288 (2008). | Article | ChemPort |
5. Smith, B. R. *et al*. Five-nanometer diamond with luminescent nitrogen-vacancy defect centers. Small 5, 1649–1653 (2009).
| Article | PubMed | ChemPort |
6. Tisler, J. *et al*. Fluorescence and spin properties of defects in single digit nanodiamonds. ACS Nano 3, 1959–1965 (2009). | Article | ChemPort |
7. Barnard, A. S. & Sternberg, M. Substitutional nitrogen in nanodiamond and bucky-diamond particles. J. Phys. Chem. B 109, 17107–17112 (2005).
| Article | PubMed | ChemPort |
8. Kruger, A. *et al*. Unusually tight aggregation in detonation nanodiamond: identification and disintegration. Carbon 43, 1722–1730 (2005).
| Article | ChemPort |
9. Mochalin, V. N. & Gogotsi, Y. Wet chemistry route to hydrophobic blue fluorescent nanodiamond. J. Am. Chem. Soc. 131, 4594–4595 (2009).
| Article | PubMed | ChemPort |
10. Holt, K. B. Diamond at the nanoscale: applications of diamond nanoparticles from cellular biomarkers to quantum computing. Phil. Trans. R. Soc. A 365, 2845–2861 (2007). | Article | PubMed | ChemPort |
11. Bradac, C., Gaebel, T., Naidoo, N., Rabeau, J. R. & Barnard, A. S. Prediction and measurement of the size-dependent stability of fluorescence in diamond over the entire nanoscale. Nano Lett. 9, 3555–3564 (2009).
| Article | PubMed | ChemPort |
12. Rabeau, J. R. *et al*. Single nitrogen vacancy centers in chemical vapor deposited diamond nanocrystals. Nano Lett. 7, 3433–3437 (2007).
| Article | PubMed | ChemPort |
13. Vlasov, I. *et al*. Nitrogen and luminsecent nitrogen-vacancy defects in detonation nanodiamond. Small 6, 687–694 (2010).
| Article | PubMed | ChemPort |
14. Boudou, J. P. *et al*. High yield fabrication of fluorescent nanodiamonds. Nanotechnology 20, 235602 (2009). | Article | PubMed | ChemPort |
15. Smith, B. R., Gruber, D. & Plakhotnik, T. The effects of surface oxidation on luminescence of nano diamonds. Diamond Relat. Mater. 19, 314–318 (2010). | Article | ChemPort |
16. Gaebel, T. *et al*. Photochromism in single nitrogen-vacancy defect in diamond. Appl. Phys. B 82, 243–246 (2006). | Article | ChemPort |
17. Kuno, M., Fromm, D. P., Hamann, H. F., Gallagher, A. & Nesbitt, D. J. 'On'/'off' fluorescence intermittency of single semiconductor quantum dots. J. Chem. Phys. 115, 1028–1040 (2001). | Article | ChemPort |
18. Tang, J. & Marcus, R. A. Diffusion-controlled electron transfer processes and power-law statistics of fluorescence intermittency of nanoparticles. Phys. Rev. Lett. 95, 107401 (2005). | Article | PubMed | ChemPort |
19. Stefani, F. D., Hoogenboom, J. P. & Barkai, E. Beyond quantum jumps: blinking nanoscale light emitters. Phys. Today 34–39 (February 2009).

20. Nirmal, M. *et al*. Fluorescence intermittency in single cadmium selenide nanocrystals. Nature 383, 802–804 (1996). | Article | ISI | ChemPort |
21. Hoogenboom, J. P., van Dijk, E., Hernando, J., van Hulst, N. F. & Garcia-Parajo, M. F. Power-law-distributed dark states are the main pathway for photobleaching of single organic molecules. Phys. Rev. Lett. 95, 097401 (2005). | Article | PubMed | ChemPort |
22. Mason, M. D., Credo, G. M., Weston, K. D. & Buratto, S. K. Luminescence of individual porous Si chromophores. Phys. Rev. Lett. 80, 5405–5408 (1998). | Article | ChemPort |
23. Cichos, F., von Borczyskowski, C. & Orrit, M. Power-law intermittency of single emitters. Curr. Opin. Colloid Interface Sci. 12, 272–284 (2007).
| Article | ChemPort |
24. Frantsuzov, P., Kuno, M., Janko, B. & Marcus, R. A. Universal emission intermittency in quantum dots, nanorods and nanowires. Nature Phys. 4, 519–522 (2008). | Article
25. Gomez, D. E., van Embden, J., Mulvaney, P., Fernee, M. J. & Rubinsztein-Dunlop, H. Exciton–trion transitions in single CdSe–CdS core–shell nanocrystals. ACS Nano 3, 2281–2287 (2009).
| Article | PubMed | ChemPort |
26. Zhang, K., Chang, H. Y., Fu, A. H., Alivisatos, A. P. & Yang, H. Continuous distribution of emission states from single CdSe/ZnS quantum dots. Nano Lett. 6, 843–847
(2006). | Article | PubMed | ChemPort |
27. Palosz, B. *et al*. Investigation of relaxation of nanodiamond surface in real and reciprocal spaces. Diamond Relat. Mater. 15, 1813–1817 (2006).
| Article | ChemPort |
28. Osswald, S., Yushin, G., Mochalin, V., Kucheyev, S. O. & Gogotsi, Y. Control of $sp^{(2)}/sp^{(3)}$ carbon ratio and surface chemistry of nanodiamond powders by selective oxidation in air. J. Am. Chem. Soc. 128, 11635–11642 (2006).
| Article | PubMed | ChemPort |
29. Iakoubovskii, K. *et al*. Structure and defects of detonation synthesis nanodiamond. Diamond Relat. Mater. 9, 861–865 (2000).
| Article | ChemPort |
30. Russo, S. P., Barnard, A. S. & Snook, I. K. Hydrogenation of nanodiamond surfaces: structure and effects on crystalline stability. Surf. Rev. Lett. 10, 233–239 (2003). | Article | ChemPort |
31. Morita, Y. *et al*. A facile and scalable process for size-controllable separation of nanodiamond particles as small as 4 nm. Small 4, 2154–2157 (2008).
| Article | PubMed | ChemPort |
32. Ushizawa, K. *et al*. Covalent immobilization of DNA on diamond and its verification by diffuse reflectance infrared spectroscopy. Chem. Phys. Lett. 351, 105–108 (2002). | Article | ChemPort |
33. Gruber, A. *et al*. Scanning confocal optical microscopy and magnetic resonance on single defect centers. Science 276, 2012–2014 (1997).
| Article | ChemPort |
34. Porezag, D., Frauenheim, T., Kohler, T., Seifert, G. & Kaschner, R. Construction of tight-binding-like potentials on the basis of density-functional theory—application to carbon. Phys. Rev. B 51, 12947–12957 (1995). | Article | ISI | ChemPort |

35. Barnard, A. S. & Sternberg, M. Crystallinity and surface electrostatics of diamond nanocrystals. J. Mater. Chem. 17, 4811–4819 (2007).
| Article | ChemPort |

1. Centre for Quantum Science and Technology, Department of Physics, Macquarie University, Sydney, New South Wales, 2109, Australia
2. MQ Photonics Research Centre, Department of Physics, Macquarie University, Sydney, New South Wales, 2109, Australia
3. Laser Physics Centre, Research School of Physics and Engineering, Australian National University, Australian Capital Territory, 0200, Australia
4. Department of Chemistry and Biomolecular Science, Macquarie University, Sydney, New South Wales, 2109, Australia
5. Virtual Nanoscience Laboratory, CSIRO Materials Science and Engineering, Clayton, Victoria, 3168, Australia
6. Department of Physics, University of Queensland, Brisbane, Queensland, Australia

Correspondence to: A. V. Zvyagin[2] e-mail: azvyagin@science.mq.edu.au

Correspondence to: J. R. Rabeau[1,2] e-mail: jrabeau@science.mq.edu.au